ANALYSIS OF SPATIAL AND TEMPORAL ADAPTIVE PROCESSING FOR GNSS INTERFERENCE MITIGATION

Chung-Liang Chang[1], Jyh-Ching Juang[2]

[1] Department of Electrical Engineering National Cheng Kung University, Tainan, Taiwan
Tel:(886)-6-763880 Fax:(886)-6-2763880 (E-mail: ngj567.liang@msa.hinet.net)

[2] Department of Electrical Engineering National Cheng Kung University, Tainan, Taiwan
Tel:(886)-6-2757575 Ext 62333Fax:(886)-6-2345482 (E-mail: juang@mail.ncku.edu.tw)

Abstract

The goal of this paper is to analyze, through simulations and experiments, GNSS interference mitigation performance under various types of antenna structures against wideband and narrowband interferences using spatial-temporal adaptive signal processing (STAP) techniques. The STAP approach, which combines spatial and temporal processing, is a viable means of GNSS array signal processing that enhancing the desired signal quality and providing protection against interference. In this paper, we consider four types of 3D antenna array structure – Uniform Linear Array (ULA), Uniform Rectangular Array (URA), Uniform Circular Array (UCA), and the Single-Ring Cylindrical Array (SRCA) under an interference environment. Analytical evaluation and simulations are performed to investigate the system performance. This is followed by simulation GPS orbits in interfered environment are used to evaluate the STAP performance. Furthermore, experiments using a 2x2 URA hardware simulator data show that with the removal of wideband and narrowband interference through the STAP techniques, the signal tracking performance can be enhanced.

Keywords: STAP, Uniform Linear Array, Uniform Rectangular Array, Uniform Circular Array, Single-Ring Cylindrical Array

1. Introduction

In recent year, the Global Navigation Satellite System (GNSS) has been widely used in military and civilian application to provide users with information of position, velocity, and time. Although the GPS system offers some inherent anti-jam protection [1,2], owing to its low signal power from satellite, an interference signal with enough power and adapted time/frequency signature could destroy the use of GPS signal for navigation. It is necessary to suppress the level of the interference well below the weak GPS signal. Throughout the years, many interference mitigation techniques of GPS have been developed; see, e.g., [3] [4]. These techniques are typically categorized in terms of post-correlation, pre-correlation, and antenna array techniques. A controlled rejection pattern antenna array (CRPA) is developed in [5] to provide better tolerance to various kinds of interferences. A swept CW (chirped interference) allows the capture of the carrier tracking loops for all signals despite the Doppler difference [6]. These approaches may be effective against a certain type of threats, but may not be applicable to all threats. Namely, adaptive temporal filter, like a notch filter, in a single antenna is effective against the narrowband interference, but may not be sufficient to account highly correlated or equally strong wideband co-exist interference suppression capabilities. It is because that the wideband interference can't be predicated from previous samples. The whitening filter can also used to mitigate the narrowband interference in a single antenna system [7]. The whitening filter has a benefit that it doesn't require the direction information of the desired signal. A disadvantage is that the whitening filter is not beamformer and it doesn't offer sufficient antenna gains as the other approach do. The uses of the antenna array in spatial domain can be effective against structured or wideband interferences but may ultimately run out of degree of freedom as the number of interferences increases [8][9]. Besides, when cost and sizes requirements limit the number of antenna elements, the adaptive antenna processing may not be effective to mitigate interference entirely. Consequently, it is desired to combine both spatial and temporal processing in order to archieve the interference mitigation performance.

The spatial-temporal adaptive processing (STAP) approach performs 2-D filtering on signals so as to remove narrowband interference and eliminate broadband interferences. The 2-D filter domain processing using antenna arrays have been widely discussed. In [10], different adaptive processing algorithms under an interference environment to determine the best methods available for the GPS antenna design. In [11], different adaptive processing algorithms under a interfered environment have been analyzed to determine the best methods available for the GPS antenna design. A joint and disjoint domain method of time and space processing performance under various design criteria is investigated in [12]. A challenge in the various phase antenna array structure affect to GPS receiver is also needs to be considered. Among the antenna array systems, the Uniform Linear Array (ULA) is the most common form used in spatial domain processing. However, different form ULA, the performance of the various type of antenna array structure has not been extensively studied for GPS interference mitigation system. In this paper, we address the problem and attempt to perform a performance analysis using various types of 3D antenna array structures - ULA, Uniform Rectangular Array (URA), Uniform Circular Array (UCA), and the Single-Ring Cylindrical Array (SRCA) under an interfered environment.

Historically, some adaptive antenna processing algorithms, implementations, and experiments in GPS interference mitigation have been devised [13][14]. This class relies on the existence of a reference or training sequence with in the data stream to be recovered. An experiment test bed of GPS antenna array has been described in [15]. It use of 3D digital beam steering techniques in software GPS receiver. In [16], a simplified spatial temporal adaptive processing technique has been investigated for interference mitigation. In [17], methods of power minimization and self-coherence properties have been assessed analytically and experimentally. The power minimization based space time processors in the context of anti-jam mitigation for an M code based GPS receiver utilizing a circular array is investigated in [18]. The GPS interference mitigation performance against narrowband and pseudolite interferences using adaptive spatial beamforming by way of simulation and experiments also has been reported in [19]. Other pertinent results can be found in [4] [7]. The paper analyzes the performance of various type antenna array structures in interference mitigation. It is assumed that the direction of arrival of the GPS signal can be obtained from an INS (inertial navigation system) or direction finding algorithm. An adaptive processing algorithm, block adaptive spatial-temporal beamforming [20], is adopted to adaptively adjust the filter coefficients (antenna weights) both on each antenna element and linear tapped-delay temporal filter so as to provide an interference-free component. We have investigated this issue via both simulation and experiment. The experiments were conducted using a four URA antenna receive channels that have five adaptive linear time taps per channel.

The remainder of this paper is organized as follows. Section 2 gives a description of the GPS signal structure and antenna array manifold vector model. It also briefly derived and introduced various type of antenna array structure. The algorithm for spatial-temporal processing is presented in Section 3. Section 4 provides the performance simulation result and discussions. The experiment results of the antenna array against narrow-band and wideband interferences are given in Section 5, and a short summary follows in Section 6.

2. Signal Model

In this section, the signal model in antenna array processing is described. The GPS signal employs DS-SS techniques and the navigation data is transmitted at an information bit rate of 50 bit/s. Both the C/A code and P code component are modulated by L1 carrier and the L2 carrier is only modulated by the P code. The received antenna signal is RF filtered and down-converted to IF and then sampled and quantized. The quantized signal is then fed to the parallel code and carrier-tracking loops. The received GPS signal power from the satellites is extremely weak because of the long distance to the satellites. The signals are actually far below the thermal noise floor according to the spectrum-spreading property. In GPS operation when the receiver in on the ground, the input signal-to-noise ratio (SNR) value is typically in the region of -15 to 20dB. The received signal is equal to the GPS signal plus a variety of interfering signals, including background noise, thermal noise, unintentional and intentional interference signals. For antenna array processing we consider three signal type: GPS signal, interference, and noise. The total received baseband signal at the kth sample of N antenna element can be described by

$$\begin{aligned}\mathbf{z}(k) &= \mathbf{z}_s(k)+\mathbf{z}_j(k)+\mathbf{z}_n(k) \\ &= \sqrt{P_s}\,s(k)\,\mathbf{a}^{(\ell)}_{\varphi_s,\theta_s} + \underbrace{\sum_{i=1}^{N_J}\sqrt{P_{j,i}}\,u_i(k)\,\mathbf{a}^{(\ell)}_{\varphi_{j,i},\theta_{j,i}} + \mathbf{z}_n(k)}_{\text{unwant signal}},\end{aligned} \tag{1}$$

where $\boldsymbol{z}_s$, $\boldsymbol{z}_n$, and $\boldsymbol{z}_j$ are the GPS signal, white Gaussian noise, and interference, respectively. We refer to $\boldsymbol{z}_n$ and $\boldsymbol{z}_j$ as unwanted signals and there are mutually uncorrelated. N_J is the total number of interfering signals. We assumed that each interference can be modeled as one of three types as follows: (1) continuous wave $cos(2\pi f_i k+\psi_i)$, where the f_i and ψ_i are the frequency and phase, respectively, (2) wideband cyclostationary signal, and (3) other wideband noise with limited bandwidth not exceeding that of the GPS signal. $\boldsymbol{a}^{(\ell)}_{\varphi_{j,i},\theta_{j,i}}$ and $\boldsymbol{a}^{(\ell)}_{\varphi_s,\theta_s}$ denote the steering vector with respect to GPS satellite and *i*th interfering source, respectively. The notation (ℓ), $\ell=1,2,3,4$ denote different form of steering vector. This steering vector function depends on antenna element arrangement. GPS signal is denoted by $s(k)$ which is essential the modulated C/A code that is subject to data modulation, time delay, Doppler shift, and phase variation. P_s and $P_{j,i}$ are signal power and *i*th interference power, respectively. $\boldsymbol{z}_n(k)$ is $1\times N$ complex white Gaussian noise vector with covariance matrix $\sigma^2\mathbf{I}_{N\times N}$. Thus, we can represent the spatial-temporal data samples in the form of an $NM\times 1$ matrix

$$\mathbf{Z}_{NM\times1}(k)=\left[\mathbf{z}_{1\times N}(k) \quad \mathbf{z}_{1\times N}(k+1) \quad \cdots \quad \mathbf{z}_{1\times N}(k+M-1)\right]^{\mathrm{H}}, \tag{2}$$

where *M* is the temporal filter tap number. In the following, we mainly address the problem of interference mitigation for the various type of antenna array configuration under the interference environment. In the following, we introduced the antenna array manifold vector model.

2.1 Antenna Array Manifold Vector Model

In this section, the adaptive antenna array configuration model is established and described. Consider the ULA of equispaced, isotropic with no coupling point sensor. It consists of a total N elements, equally distributed at the observation angle (φ,θ). The steering vector function of the signal for the azimuth, φ and elevation, θ can be defined as:

$$\mathbf{a}^{(1)}_{\varphi,\theta}=\left[1 \quad e^{jkd_xu} \quad \cdots \quad e^{jkNd_xu} \quad e^{jk(N\text{-}1)d_xu}\right]^{\mathrm{H}} \tag{3}$$

where $k=2\pi/\lambda$ is the free-space wave number at some IF frequency, λ is the working wavelength, $u=sin(90^\circ-\theta)cos(90^\circ-\varphi)$, and d_x is the inter-element spacing along the x direction. The notation $[\bullet]^{\mathrm{H}}$ denotes the Hermitian transpose operation. For a two-dimensional URA in which all antenna elements are assumed to be isotropic with no couplings, there are $P\times Q$ elements in the array and each element using phase steering at the (p,q) location to place the beam peak. The steering vector at the observation angle (φ,θ) is given by the following:

$$\mathbf{a}_{\varphi,\theta}^{(2)} = \Big[1 \;\; e^{jkd_y v} \;\; \cdots \;\; e^{jk(Q\text{-}1)d_y v} \;\; \cdots \;\; e^{jkd_x u} \;\; e^{jk(d_x u + d_y v)} \;\; e^{jk(d_x u+(Q\text{-}1)d_y v)} \;\; \cdots \;\; e^{jk(d_x (P\text{-}1)u)} \;\; \cdots \;\; e^{jk(d_x (P\text{-}1)u+(Q\text{-}1)d_y v)}\Big]^{H} \quad (4)$$

where $v = sin(90^{\circ} - \theta)cos(90^{\circ} - \varphi)$, and d_y is the inter-element spacing along the y direction.. The circular array pattern of radius r with total N elements at each element locations $\varphi' = n\Delta\varphi,\ n = 1,2,...,N$ can be written as

$$\mathbf{a}_{\varphi,\theta}^{(3)} = \Big[e^{jkrsin(90^{\circ}\text{-}\theta)cos(90^{\circ}\text{-}(\varphi\text{-}\Delta\varphi))} \;\; e^{jkrsin(90^{\circ}\text{-}\theta)cos(90^{\circ}\text{-}(\varphi\text{-}2\Delta\varphi))} \;\; \cdots \;\; e^{jkrsin(90^{\circ}\text{-}\theta)cos(90^{\circ}\text{-}(\varphi\text{-}(N\text{-}1)\Delta\varphi))} \;\; e^{jkrsin(90^{\circ}\text{-}\theta)cos(90^{\circ}\text{-}(\varphi\text{-}N\Delta\varphi))}\Big]^{H}, \quad (5)$$

where the first element is assumed to locate at the x-axis direction of the coordinate system as the phase reference point. A particular type of conformal array antennas for the military and communications systems is multi ring cylindrical array. A sector array of elements is "turned on" in order to create a radically outward antenna beam. The beam is scanned around 360 degrees by consecutively exciting adjacent sectors of elements. The geometry of a typical cylindrical array is also considered in wh ich the resulting equation for the steering vector of the k^{th} loop with each nk elements located at equally spaced angles $\varphi_{nk} = n\Delta\varphi_k$ is given by：[21]

$$\mathbf{a}_{\varphi,\theta}^{(4)} = \begin{bmatrix} e^{jk\left[r_1 sin(90^{\circ}\text{-}\theta)cos(90^{\circ}\text{-}(\varphi\text{-}\Delta\varphi_{11}))+z_1 sin(90^{\circ}-\theta)\right]} \\ \vdots \\ e^{jk\left[r_1 sin(90^{\circ}\text{-}\theta)cos(90^{\circ}\text{-}(\varphi\text{-}N\Delta\varphi_{n1}))+z_1 sin(90^{\circ}-\theta)\right]} \\ e^{jk\left[r_2 sin(90^{\circ}\text{-}\theta)cos(90^{\circ}\text{-}(\varphi\text{-}\Delta\varphi_{12}))+z_2 sin(90^{\circ}-\theta)\right]} \\ \vdots \\ e^{jk\left[r_2 sin(90^{\circ}\text{-}\theta)cos(90^{\circ}\text{-}(\varphi\text{-}N\Delta\varphi_{n2}))+z_2 sin(90^{\circ}-\theta)\right]} \\ \vdots \\ e^{jk\left[r_k sin(90^{\circ}\text{-}\theta)cos(90^{\circ}\text{-}(\varphi\text{-}N\Delta\varphi_{nk}))+z_k sin(90^{\circ}-\theta)\right]} \end{bmatrix}_{Nk\times 1} \quad (6)$$

In this work, the single-ring cylindrical array is considered. The goal of this paper is to determine the weight function that optimizes the broadside pattern directivity. In the following, we introduced the adaptive antenna processing.

3. Adaptive Antenna Processing

In this section we investigate several spatial-temporal filter methods for GPS interference mitigation processing. The design guideline of adaptive antenna algorithm can be imposed at spatial domain or temporal domain. In this paper, we select various type of adaptive antenna algorithm to impose the spatial and temporal filter under several antenna array configurations. The adaptive algorithms are in the form of conventional match filtering (CMF), minimum variance distortion less response (MVDR) [20], and extended block adaptive spatial beamforming (EBASB) [19] approach.

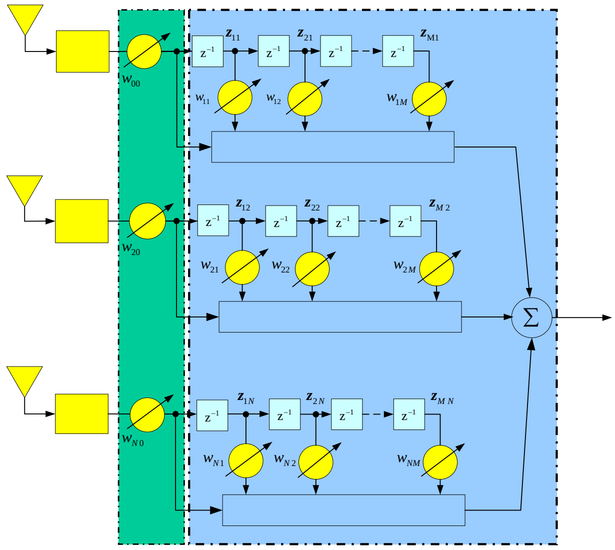

Figure 1. Block diagram of antenna array system

Figure 1 show the block diagram of spatial-temporal antenna array system. The optimal adaptive weights are computed using the various adaptive algorithms. The measurement data are multiplied by the adaptive weights and summed up to give the output for acquisition/tracking applications. Suppose that the desired signal is given by $d(k,\varphi_s,\theta_s)$ and the objective function to be minimized is

$$E\left\{\left\|y(k) - d(k)\right\|^2\right\} \quad (7)$$

Let $\mathbf{w}_{\text{CMF\_st}}$ be an observation vector consisting of a total of NM measurements that can conveniently be represented by the Kronecker product [22] of the spatial and temporal steering vectors, namely,

$$\mathbf{w}_{\text{CMF\_st}} = \mathbf{b} \otimes \mathbf{a}_{\varphi,\theta}^{(\ell)} / N \quad (8)$$

where $\mathbf{w}_{\text{CMF\_st}}$ is the NM -dimensional spatial-temporal steering vector, where $\mathbf{b}$ and $\mathbf{a}_{\varphi,\theta}^{(\ell)}$ is its corresponding M -dimensional temporal steering vector and N -dimensional spatial steering vector of the signal of interest, respectively. It is the least-square optimal weight vector solution of Conventional Matched-Filter (CMF) [23]. The scale $1/N$ preserves the energy of the signal of interest at the output. The superscript (ℓ) denotes the different form of antenna array configuration. Then the output of the antenna array system becomes

$$y_{\text{CMF}}(k) = \mathbf{w}_{\text{CMF\_st}}\, \mathbf{Z}(k) \quad (9)$$

where $\mathbf{Z}(k)$ is as in Eq. (2) which can be decomposed into three components: signal, interference, and noise are given by:

$$\mathbf{Z}_{NM\times 1}(k) = \mathbf{Z}_s(k) + \mathbf{Z}_j(k) + \mathbf{Z}_n(k) \quad (10)$$

The first measure we will consider is the interference-plus-noise ratio after adaptation, is given by

$$\mathrm{INR} = \frac{\mathrm{E}\left\{\left\|\mathbf{w}^{\mathrm{H}}\mathbf{Z}_j\right\|^2\right\}}{\mathrm{E}\left\{\left\|\mathbf{w}^{\mathrm{H}}\mathbf{Z}_n\right\|^2\right\}} \tag{11}$$

A second measure is the signal-to-interference-plus-noise ratio after adaptation, as given by

$$\mathrm{SINR} = \frac{\mathrm{E}\left\{\left\|\mathbf{w}^{\mathrm{H}}\mathbf{Z}_s\right\|^2\right\}}{\mathrm{E}\left\{\left\|\mathbf{w}^{\mathrm{H}}\mathbf{Z}_j\right\|^2\right\}+\mathrm{E}\left\{\left\|\mathbf{w}^{\mathrm{H}}\mathbf{Z}_n\right\|^2\right\}} \tag{12}$$

where $\mathbf{Z}_s$, $\mathbf{Z}_j$, and $\mathbf{Z}_n$ are given by Eq. (1). Another adaptive processing algorithm is minimum variance distortion less response (MVDR). The MVDR technique is used to suppress the interference and noises by constraining the response of the beamformer to specific directions and then minimizing the output power subject to the response constraints. If we assumes that the direction of signal of interest is known. The spatial-temporal MVDR optimal solution is given by the following expression:

$$\mathbf{w}_{\mathrm{MVDR\_st}} = \frac{\mathbf{M}^{-1}\mathbf{w}_{\mathrm{CMF\_st}}}{\mathbf{w}^{\mathrm{H}}_{\mathrm{CMF\_st}}\mathbf{M}^{-1}\mathbf{w}_{\mathrm{CMF\_st}}} \tag{13}$$

where $\mathbf{M}$ is the MN -by- MN covariance matrix of the spatial-temporal data input vector. Another adaptive algorithm is extended block adaptive spatial beamforming algorithm (BASB) [19]. Some manipulations reveal that the optimal weighting vector is given by [13] [14].

$$\mathbf{w}_{\mathrm{BASB\_st}} = \left(\mathbf{Z}^{\mathrm{H}}(k)\mathbf{Z}(k)\right)^{-1}\mathbf{Z}^{\mathrm{H}}(k)d(k) \tag{14}$$

In the Block Adaptation Spatial Beamforming with Memory (BASB-M), the correlation matrix and weighting vector computed with respect to the previous block is utilized and the new weighting vector is updated in accordance with

$$\mathbf{w}_{\mathrm{BASB\_st}}(k) = \mu\mathbf{w}(k\text{-}1)+(1-\mu)\left(\mathbf{Z}^{\mathrm{H}}(k)\mathbf{Z}(k)\right)^{-1}\mathbf{Z}^{\mathrm{H}}(k)d(k) \tag{15}$$

where μ is a scalar between 0 and 1.

4. Numerical Simulation

In this section, computer simulations are conducted to assess the performance of the proposed methods under different form of antenna array configuration. For various array configurations, two case of simulation are considered. Two cases encompass narrowband interference and wideband interference. The first case involved four wideband interference and one narrowband interference. The second case included four narrowband interference and one wideband interference. Figure 2 plot the magnitude of the multi-dimensional Fourier Transform of the spatial-temporal weights of the URA with a half of wavelength spacing in case 1 and case 2, respectively. For case 1, Figure 2(a) displays a well-defined null along the arrival angle of four wideband interferences. For case 2, Figure 2 (b) displays a well-defined null at the angle frequency coordinate of narrowband interference. The SINR improvement against different adaptive array algorithm and configuration are summarized in Table 1. The SINR improvement is defined as the difference between the output SINR and input SINR. The output SINR is a function of after the adaptive processing. In Table 1, we can observe that the SINR improvement due to EBASB-M method have the best performance than others for case 1. In case 2, the MVDR method outperforms others. Thus, we propose to use URA structure by getting the better SINR improvement under the same antenna elements. Observe that use URA structure to all have better SINR improvement under different adaptive algorithm. However, the SCRA just only 5 antenna element be used, thus cause its SINR improvement is not good. Come to say wholly, under the same array element and tap number, adaptive algorithm to the narrowband interference mitigation performance better than wideband interference mitigation performance. In Figure 3 we show a typical result for the signal correlation as a function using EBASB-M approach under the different array configuration.

Table 1. (Antenna element = 9, tap = 5)

Adaptive algorithm		SINR improvement (dB)			
		ULA	UCA	URA	SRCA
CMF	case 1	19.4	19.8	20.8	13.4
	case 2	21.6	21.6	21.6	13.1
MVDR	case 1	37.7	39.0	40.2	31.6
	case 2	42.1	42.5	44.5	30.9
EBASB-M	case 1	38.0	39.6	41.3	31.5
	case 2	41.1	42.0	43.9	30.7

There is no discernable displacement of the correlation function peak from its correct location at zero code phase offset in Figure 3. Moreover, the cross correlation function of Figure 3 (a) has nearly the same shape in the presence of interference in case1 as it does in the interference of Figure 3(b) of case 2 using URA structure. Even in the present of several strong wideband or narrowband interference, there is not a drastic broadening of the correlation function. Therefore, the increase in pseudo-range error is limited. It is found that the URA structure can obtain the best correlation function in all cases. But for SCRA configuration there is a significant broadening of the correlation peak. This is because the SRCA only five antenna element can utilize to against stronger interference.

5. Test Hardware and Experiments Results

Based on the aforementioned simulation results, a uniform rectangular array with four GPS patch antennas is implemented. The distance between antenna elements is half-wavelength of the GPS L1 signal. Four commercial GPS front-ends are used to filter, down-convert, and digitize incoming RF signal to give digital samples. A master clock is used to control the synchronization among four different channels so that the samples are obtained at the same time as possible. The IF frequency of each front end is 4.092MHz, the sampling rate is 16.368MHz, and ADC performs 2-bit quantization.

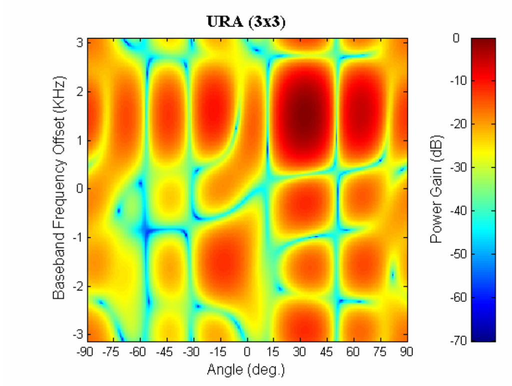

(a)

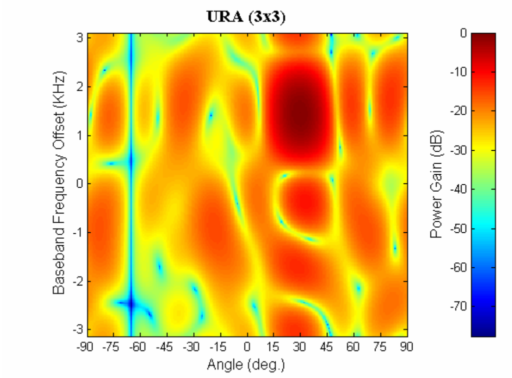

(b)

Figure 2. (a) AOA frequency response (URA): 4WBI, 1NBI. (b) AOA frequency response (URA): 4NBI, 1WBI.

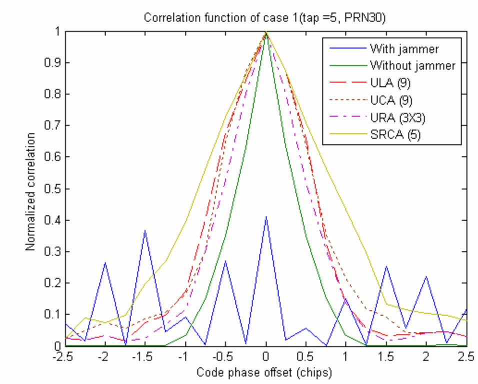

(a)

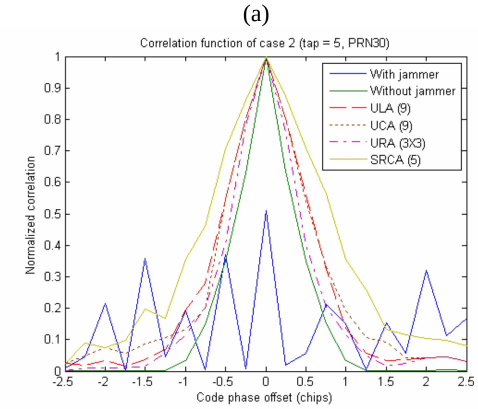

(b)

Figure 3. Code phase delay v.s Normalized correlation: (a) case1 (b) case2.

The digital samples are acquired by a PCIbased data acquisition board (PCI-6534) through data acquisition software (NI LabView). The data samples from each antenna element are stored and, afterwards, post processed for interference mitigation analysis. The observable GPS satellites are depicted in the sky plot of Figure 4. The figure also illustrates the location of the interferer which is located at azimuth 315° and elevation 10°. There are seven GPS satellites being observed. The interferer is then switched on and the data that contain components due to GPS satellites, the interferer, and noises are recorded. A 60ms data record was collected using the four channels and EBASB-M algorithm with five tap are used to process the data which is sampled at 16.368 MHz. Each block data size is thus selected as 16368 so that a 1-msec data constitute one block. In the post-processing stage, the acquisition results with and without the applications of the adaptive spatial-temporal algorithm are analyzed. Again, two types of interferences are considered in the experiment. One is the pseudolite-type interference and the other is continuous-wave interference. The former is generated by an indigenously developed dual-frequency pseudolite [24] and the latter is generated using a signal synthesizer. For combined wideband (pseudolite-type) and narrowband interference experiment case, both the ISR are again 30 dB, respectively. In this test, when the WBI and NBI has not been turned on, the satellite with PRN 25 cannot be successfully tracked as its signal acquisition margin (SAM) [19] is below the threshold value which is set at 5 dB. The other satellites with PRN 5, 14, 15, 18, 30, and 22, respectively, can be tracked. When the WBI is turned on, all GPS satellites become unlocked. After the application of the spatial-temporal adaptive algorithm (BASB-M), the GPS satellites can all be acquired again with acceptable SAM as tabulated in Table 2. Figure 5 illustrate the antenna pattern as the adaptive algorithm (E BASB-M) null the interference. The adaptive spatial-temporal processing also brings another benefit in this case as the GPS satellite with PRN 25 can be acquired after the spatial-temporal adaptive processing. However, the satellite with PRN 15 cannot be locked even when adaptive algorithm is applied. This may be attributed to its low elevation.

Table 2. NBI and WBI effect to GPS signal acquisition

ISR = 30 dB			
SAM (detection threshold = 5 dB, tap = 5)			
PRN	Before WBI and NBI on	After WBI and NBI on	After STAP
22	7.64	-	7.51
14	6.23	-	5.11
18	7.21	-	9.81
30	7.14	-	8.31
15	5.87	-	-
5	6.02	-	5.32
25	-	-	5.01

6. Conclusion

In this paper, a spatial-temporal adaptive antenna approach is adopted for the mitigation of interferences for GNSS navigation. Three different realizations of the spatial-temporal adaptive beamforming algorithm are assessed under different interference conditions, array configuration, and steering vector mismatch. Among three realizations, the EBASB-M algorithm results in the best SINR improvement. It was demonstrated that the uniform rectangular array configuration has advantages over others. Finally, an array is henceforth implemented and tested against wideband (pseudolite-type) and narrowband interference. The interference mitigation performance is experimentally verified. With respect to narrowband and wideband interference, the 2x2 array is capable of withstanding up to 30 dB ISR.

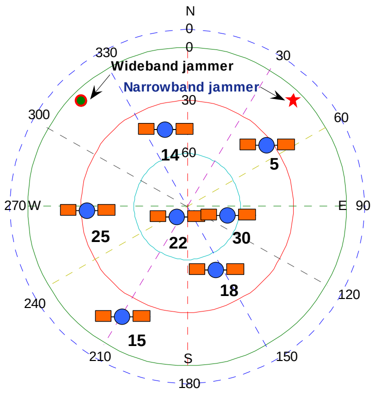

Figure 4. Sky plot of GPS satellite and interference.

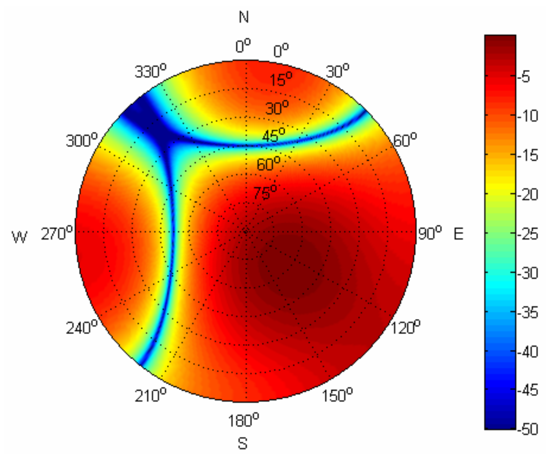

Figure 5. Azimuth and elevation antenna gain pattern for a four channel system.

Acknowledgement

This work was supported by the National Science Council, Taiwan, R.O.C. under Grant NSC-95-2221-E-006-365.

Reference

1. E. D. Kaplan, *Understanding GPS: Principle and Application*, Artech House, London, 1996.
2. B. W. Parkinson and J. J. Spilker, *Global Positioning System: Theory and Applications*. Washington, DC: AIAA, 1996.
3. J. J. Jr. Spilker, and F. D. Natali, "Interference Effects and Mitigation Techniques," in B. W. Parkinson et al (eds.) *Global Positioning System: Theory and Applications*, American Institute of Aeronautics and Astronautics, 1996, pp. 717-772.
4. P. Ward, "Effects of RF Interference on GPS Satellite Signal Receiver Tracking," in E. D. Kaplan (ed.) *Understanding GPS: Principles and Applications*, Artech House, Norwood, 1996, pp. 209-236.
5. W. Kunysz, "Advanced Pinwheel Compact Controlled Reception Pattern Antenna designed for Interference and Multipath Mitigation, " *Proceedings of ION GPS 2001*, Salt Lake City, UT, September 11-14, 2001, pp. 2030-2036.
6. H. Johnston, "A Comparison of CW and Swept CW Effects on a C/A Code GPS Receiver," *Proceedings of ION GPS 1997*, Kansas City, MO, September 16-19, 1999, pp. 149-158.
7. J. W. Ketchum and J. G. Proakis, "Adaptive Algorithm for Estimating and Suppressing Narrow-band Interference in PN Spread-Spectrum Systems, " *IEEE Transactions on Communications*, Vol. 30, No. 5, pp. 913-924, 1982.
8. T. Upadhyay, et al., "Test Results on Mitigation of SATCOM-Induced Interference to GPS Operation," *Proceedings of the ION GPS-95 Conference*, September 1995, pp. 1545-52.
9. D. J. Moelker, et al., "Adaptive Antenna Arrays for Interference cancellation in GPS and GLONASS receivers," *Proceedings of the IEEE Position, Location and Navigation Symposium*, April 1996, pp. 191-198.
10. J. Vaccaro and R. Fante, "Ensuring GPS Availability in an Interference Environment," *Proceedings of ION GPS 2000*, Salt Lake City, UT, September 19-22, 2000, pp. 458-461.
11. I. Gupta and Moore T., "Space-Frequency Adaptive Processing for Interference Suppression in GPS Receivers," *Proceedings of ION NTM 2001*, Long Beach, CA, January 22-24, 2001, pp. 377-385.
12. X. Ping, J. M. Michael, N. B. Stella, "Spatial and Temporal Processing for Global Navigation Satellite System: The GPS Receiver Paradigm," *IEEE Trans. on Aerospace and Electronic Systems*, Vol. 39, No. 4, 2003, pp.1471-1484.
13. S. Haykin, *Array Signal Processing*, Prentice Hall, Englewood Cliffs, NJ, 1985.
14. S. Hyakin, Adaptive Filter Theory, 3rd Ed., Prentice Hall, Englewood Cliffs, 1996.
15. K. Gold, R. Silva, R. Worrell, and A. Brown, "Space Navigation with Digital Beam Steering GPS Receiver Technology," *in Proc. ION Annual Meeting*, Albuquerque, NM, 2003.
16. R. L. Fante and J. J. Vaccaro, "Wideband Cancellation of Interference in a GPS Receiver Array," *IEEE Trans. on Aerospace and Electronic Systems*, Vol. 36, No. 2, 2000, pp. 549-564.
17. Y. T. J. Morton, L. L. Liou, D. M. Lin, J. B. Y. Tsui, and Q. Zhou, "Interference Cancellation Using Power Minimization and Self-Coherence Properties of GPS Signals, " *in Proc. ION GNSS Conf.*, Long Beach, CA, 2004.
18. W. L. Myrick, J. S. Goldstein, and M. D. Zoltowski, "Low Complexity Anti-jam Space-Time Processing for GPS, " *Proceeding of the 2001 IEEE International Conference on Acoustics, Speech, and Signal Processing*, Salt Lake City, UT, M ay 2001, pp. 2233-2236.
19. J. C. Juang and C. L. Chang, "Performance Analysis of GPS Pseudolite Interference Mitigation Using Adaptive Spatial Beamforming," *Proc. ION Annual Meeting*, Boston, 2005.
20. C. Tang, K. Liu, S. Tretter, "Optimal Weight Extraction for A daptive Beamforming using Systolic Arrays, " *IEEE Transactions on Aerospace and Electronic System*, Vol. 30, No. 2, April 1994.
21. R. J. Mailloux, *Phased Array Antenna Handbook, Massachusetts: Artech House*, Norwood MA, 1994.
22. M. Zatman, "Production of Adaptive Array Troughs Through Dispersion Synthesis," *Electronics Letters*, Vol. 31, No. 25, December 1995, page 2141.
23. P. Misra, B. P. Burke, and M. M. Pratt, "GPS Performance in Navigation," *Processing of the IEEE*, January 1999, pp. 65-85.
24. J. C. Juang, K. Y. Cheng, C. L. Tseng, and C. F. Lo, "The Design and Test of a Dual-Frequency GPS Pseudo-Satellite Augmentation System," *in Proc. Int. Conference. on Integrated Navigation Systems*, Saint Petersburg, Russia, 2004.